https://doi.org/10.5194/egusphere-2023-1913
Preprint. Discussion started: 26 September 2023

Stream hydrology controls on ice cliff generation, evolution, and survival on debris-covered glaciers

Eric Petersen[1], Regine Hock[2,1], and Michael G. Loso[3]

[1]Geophysical Institute, University of Alaska Fairbanks, Fairbanks, AK, USA
[2]Department of Geosciences, University of Oslo, Oslo, Norway
[3]Wrangell-St. Elias National Park and Preserve, National Parks Service, Copper Center, AK, USA

Correspondence: Eric Petersen (eipetersen@alaska.edu)

Abstract. Ice cliffs are melt hot spots that contribute disproportionately to melt on debris-covered glaciers. In this study, we investigate the impact of supraglacial stream hydrology on ice cliffs using in-situ and remote sensing observations, stream flow measurements, and a conceptual geomorphic model of ice cliff backwasting applied to ice cliffs on Kennicott Glacier, Alaska. We found that 31.4% of ice cliffs are actively influenced by streams, while 46.4% are less than 10 m from the nearest stream. Supraglacial streams contribute to ice cliff formation and maintenance by horizontal meandering, vertical incision, and debris transport. Meander morphology reminiscent of sedimentary river channel meanders and oxbow lakes leads to sinuous or crescent-shaped ice cliff shapes. Stream action at the base of ice cliffs aids in cliff maintenance by enhancing incision and preventing reburial. These processes produce an undercut lip and transport clasts up to tens of centimeters in diameter. Stream avulsions result in rapid ice cliff collapse and local channel abandonment. Ice cliffs abandoned by streams are observed to be reburied by supraglacial debris, indicating a strong role played by streams in ice cliff persistence. The development of landscape evolution models may assist in quantifying the total net effect of these processes on steady state ice cliff coverage and mass balance on debris-covered glaciers.

1 Introduction

Glaciers covered extensively by rocky debris are found worldwide but are most common in High Mountain Asia, Alaska, and the Central Andes where glaciers are key contributors to glacial melt and regional freshwater resources (Scherler et al., 2018; Herreid and Pellicciotti, 2018; Bhushan et al., 2018). It is thus critical for these regions to have a firm understanding of the effect supraglacial debris has on surface melt.

Supraglacial debris exhibits a strong control on glacier melt which is empirically described by the Østrem curve (Østrem, 1959). Thin debris cover increases melt relative to a bare ice surface, but a sufficiently thick debris layer (typically on the order of a few centimeters for rocky debris) attenuates melt significantly in a non-linear fashion (Østrem, 1959; Khodakov, 1972; Dolgushin, 1972; Bozhinskiy et al., 1986; Mattson et al., 1993). Debris-covered glaciers are defined by the development of continuous debris cover across much of their ablation zone (Cogley et al., 2011), with debris commonly thick enough to retard ablation and lead to the development of a stagnant tongue of ice with a delayed response to climatic forcing (Benn et al., 2012; Bolch et al., 2012; Mölg et al., 2020; Anderson and Anderson, 2016).

https://doi.org/10.5194/egusphere-2023-1913
Preprint. Discussion started: 26 September 2023

Ice cliffs, where the glacier surface is sufficiently steep to shed itself locally of debris, contribute significantly to melt on debris covered glacier surfaces (Sakai et al., 2002; Buri et al., 2021; Anderson et al., 2021a). Some studies have suggested that they may contribute to the "debris-cover anomaly" which describes the observation that area-averaged melt rates are comparable for debris-covered and non-debris covered portions of glaciers at similar elevations, despite the localized attenuation of melt by thick debris cover (Kääb et al., 2012; Gardelle et al., 2013; Pellicciotti et al., 2015; Maurer et al., 2019). Thus, it is of importance to understand and capture ice cliffs in models of retreat for debris-covered glaciers.

Controls on ice cliff formation, evolution, and survival are an area of intensifying research (Kneib et al., 2023; Sato et al., 2021; Buri and Pellicciotti, 2018; Anderson et al., 2021a). Differential melt under variable debris thickness creates rough surface topography (Anderson, 2000; Moore, 2021); ice cliffs may be generated where the surface is sufficiently steep to slough debris. Ice cliffs may also be produced as a result of modified crevasses, from the incision of supraglacial streams, from the collapse of englacial voids resulting in exposed ice walls (Mölg et al., 2020), or be associated with the rims of supraglacial ponds (Scott Watson et al., 2017). Buri and Pellicciotti (2018) showed that aspect is a strong control on cliff survival; ice cliffs with a poleward aspect tend to persist whereas ice cliffs with an equatorward aspect tend to flatten as a result of differential insolation-driven melt, and are reburied.

A number of studies have suggested a strong relationship between ice cliffs and supraglacial streams. Mölg et al. (2020) noted on Zmuttgletscher the presence of "cryo-valleys" carved into the debris-covered surface by supraglacial streams, with ice cliffs formed in the resulting high relief. Anderson et al. (2021b) noted that ice cliffs often act as initiation points for supraglacial streams due to their role as a locally enhanced melt water source. Sato et al. (2021) reported a correlation between active supraglacial stream networks and the presence of new ice cliffs, suggesting a causative link. Kneib et al. (2023) noted that 38.9% of ice cliffs surveyed on 86 glaciers in High Mountain Asia were associated with supraglacial streams, while 19.5% were associated with supraglacial ponds. This highlights a close relationship between ice cliffs and hydrology, particularly stream hydrology.

In this study, we examined in detail the links between ice cliffs and supraglacial stream hydrology on Kennicott Glacier, Alaska. We performed analysis on a photogrammetric dataset (September 2018) and in-situ observations (summer field seasons 2020-2022), and developed a conceptual geomorphic model of ice cliff backwasting to examine stream impacts on ice cliff development. We also describe the results of stream gauging to determine the ability of streams to erode transport supraglacial debris.

https://doi.org/10.5194/egusphere-2023-1913
Preprint. Discussion started: 26 September 2023

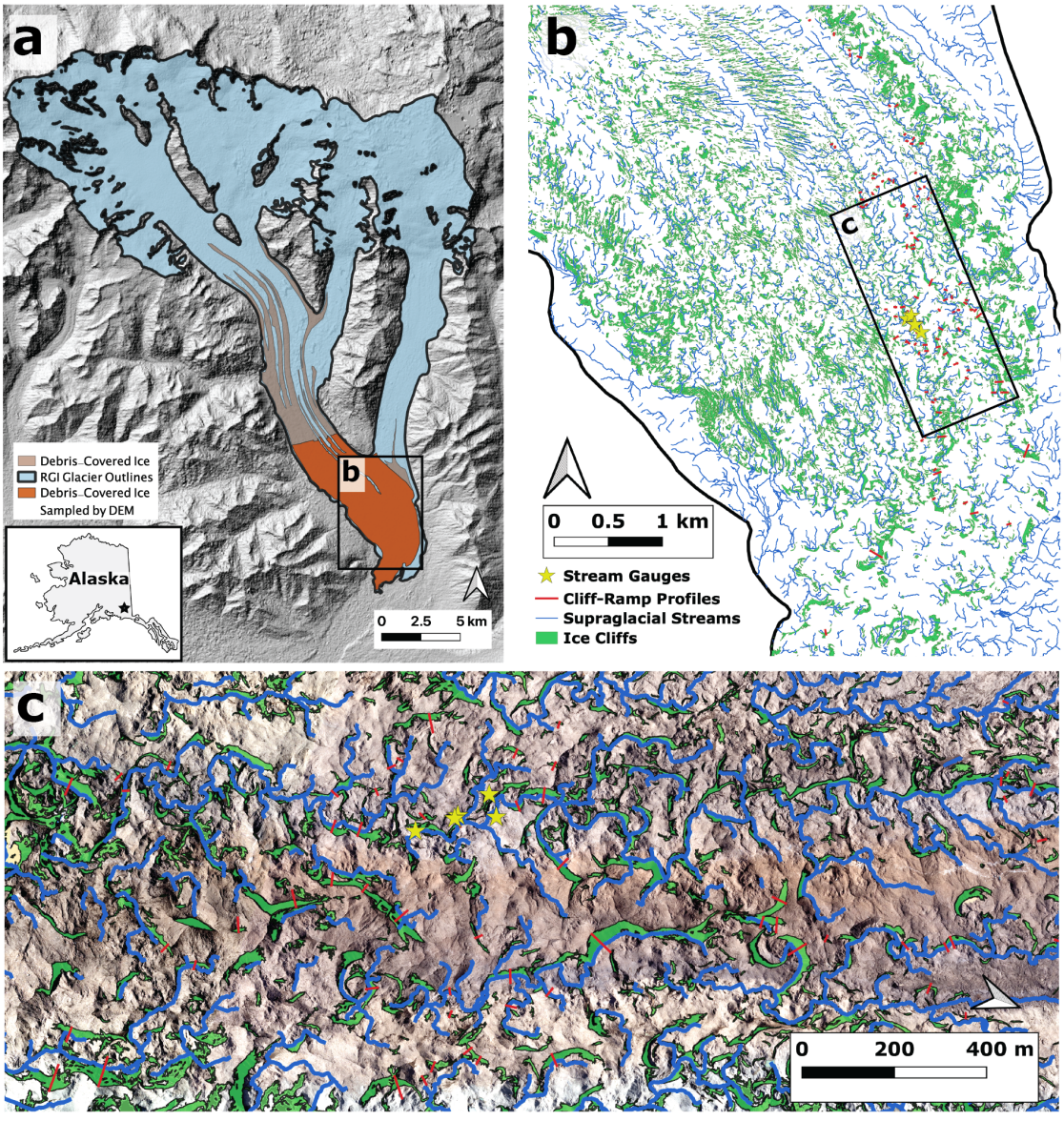

Figure 1. (a) Kennicott Glacier and tributaries with Randolph Glacier Inventory (RGI) outlines (RGI Consortium, 2017) mapped on an ASTER (Advanced Spaceborne Thermal Emission and Reflection Radiometer) DEM hillshade (NASA/METI/AIST/Japan Spacesystems and U.S./Japan ASTER Science Team, 2019). Debris-covered area as well as the area sampled by the NPS airborne photogrammetry DEM is mapped. (b-c) Delineated ice cliffs and stream channels (both predicted from DEM analysis) as well as the location of discharge measurements. Panel (c) includes NPS airborne photogrammetry orthophoto as a basemap. Note that there is some error in the mapped RGI outline; moraine and glaciofluvial deposits have been falsely identified as glacier, particularly for the southeast portion of the terminus (we have omitted these areas in our map of the glacier's debris-cover).

https://doi.org/10.5194/egusphere-2023-1913
Preprint. Discussion started: 26 September 2023

2 Study Site

Kennicott Glacier is a 43 km long valley glacier located in Wrangell-St. Elias National Park, Alaska (Figure 1). It flows from the southern flank of Mount Blackburn at 4996 m a.s.l. to its terminus at ∼400 m a.s.l. (RGI Consortium, 2017). Nine medial moraines grow and merge down glacier, causing the formation of a continuous supraglacial debris layer ∼7 km from the terminus. One study (Anderson et al., 2021a) determined that 20% of Kennicott Glacier's surface is debris-covered, while 26% of determined melt rates in summer 2011 were attributed to ice cliffs covering 12% of the glacier's terminus region (lowermost 8.5 km).

3 Methods

3.1 Ice cliff and stream mapping using photogrammetry

A photogrammetric dataset was flown on September 13, 2018 over the debris-covered terminus of Kennicott Glacier, covering its surface from the confluence with the Root Glacier to the toe. 1691 images were taken using a Nikon D850 with a 24mm prime lens at an average flying altitude of 940 m. These images were processed using Agisoft Metashape to produce a digital elevation model (DEM) at 0.32 m resolution and an orthophoto at 0.16 m resolution. Four ground control points were surveyed at the McCarthy airport to calibrate the final DEM product, resulting in a +0.13 m vertical adjustment to the ellipsoidal heights. The photogrammetric dataset covers 33.8 km^2 (37.2 km^2 when corrected for slope) of the total 54.8 km^2 of debris-covered ice on Kennicott Glacier, and extends up to an elevation of 830 m on the glacier surface (coverage mapped in Figure 1a).

Ice cliffs were identified from the DEM in the following way. (1) Grid cells with slope angles greater than $> 30°$ were isolated in a mask. (2) This mask was converted to a shapefile with contiguous collections of grid cells as individual shapes. (3) Gaps < 10 m^2 in size contained entirely within ice cliff shapes were filled. (4) Slope statistics on ice cliff shapes were calculated and shapes with maximum slope of $< 50°$ were removed from the inventory. The final step was employed to reduce false ice cliff detection where the debris-covered surface may be steepened but not yet shed of debris, with the $50°$ cutoff chosen based on visual confirmation of random samples at different maximum slope values.

To prepare the DEM for hydrologic analysis, it was downsampled to 2 m resolution. Supraglacial streams often undercut ice cliffs and are thus not visible in the top-down view of the photogrammetry dataset; debris mounds which the stream channel meanders around (via ice cliff undercut) may be seen as hydrologic obstructions. For this reason sinks < 3 m in depth were filled in the DEM; this value was chosen as a cutoff based upon the typical roughness of debris-covered ice within stream corridors observed in the field on Kennicott Glacier. Stream channels were then predicted over the modified DEM by using the Channel Network tool in SAGA-GIS; this tool calculates runoff catchment area for each pixel in the DEM and returns channels defined by contiguous pixels with catchment area greater than a set threshold, defined in this case as 2500 m^2. The chosen threshold was somewhat arbitrary, but represents a potential channel flow of 1200-2300 cm^3 s^{-1} (assuming a mean sub-debris melt rate of 4 - 8 cm per day and ignoring ice cliffs). Note that these are predicted channels, and may not necessarily be filled with melt water in all cases.

https://doi.org/10.5194/egusphere-2023-1913
Preprint. Discussion started: 26 September 2023

To determine spatial proximity between supraglacial streams and ice cliffs, point shapefiles were generated representing stream lengths and ice cliff areas at 2 m resolution. For each 2 m length of stream, the distance to the nearest ice cliff point was then determined.

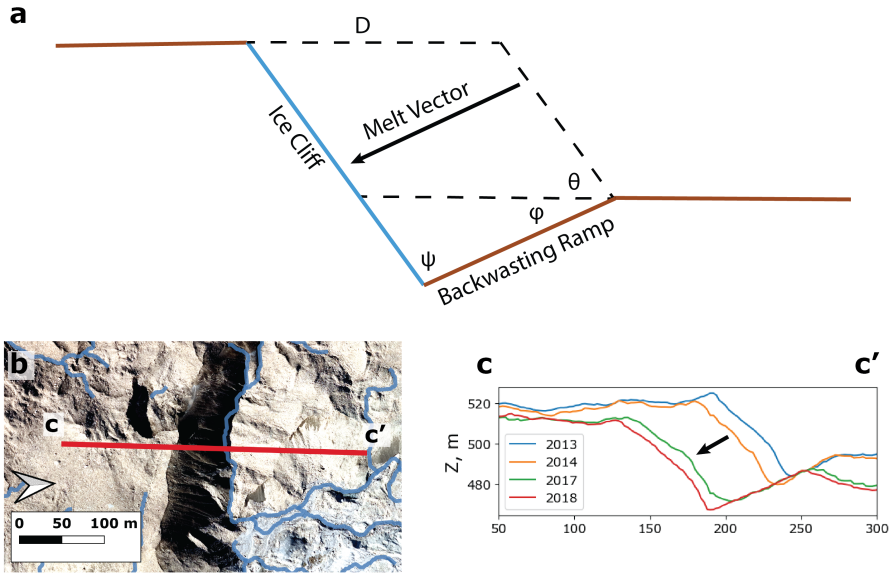

Figure 2. (a) Conceptual model for the geometry of ice cliff backwasting. The melt vector is orthogonal to the exposed ice surface (angle θ from the horizontal), thus there is a component of vertical incision in addition to horizontal backwasting. The ice cliff as it back wastes produces a ramp of angle ψ to itself and ϕ to the horizontal. The value of the angle ψ indicates the efficiency of incision. (b) Map illustrating the location of profile c-c' over a large ice cliff associated with a supraglacial stream (mapped as blue lines). (c) Topographic profiles extracted from ArcticDEM illustrating the backwasting of the ice cliff and the carving out of the backwasting ramp. This ice cliff has an angle between cliff and ramp of ψ = 110°. This ice cliff is in the glacier's stagnant terminus region where surface velocity is negligible and thus did not need to be deconvolved from the signal of surface change.

3.2 Geomorphic model of ice cliff backwasting

We developed an idealized geomorphic model of ice cliff backwasting in order to analyze the effect of streams on ice cliffs as recorded in the DEM. This model focuses on the relationship between ice cliffs and their "backwasting ramps." We define a backwasting ramp as the slope on a debris-covered glacier surface generated by the ice cliff melting vertically as well as horizontally into the surface of the glacier. Backwasting ramps have not previously been identified in the literature.

Consider an ice cliff at an angle of θ that backwastes through a two-dimensional debris-covered glacier surface (Figure 2a). Backwasting is driven by melt orthogonal to the ice cliff face. Thus, as the ice cliff melts at a rate M it produces vertical incision ($Mcos(\theta)$) as well as horizontal wasting ($Msin(\theta)$), and scours out a backwasting ramp at an angle of $\pi/2$ from the ice cliff and $\phi = \pi/2 - \theta$ from the horizontal. However, incision at the base of the ice cliff is not expected to be fully efficient,

https://doi.org/10.5194/egusphere-2023-1913
Preprint. Discussion started: 26 September 2023

due to the effects of differential insolation-driven ablation and reburial by debris. The presence of streams may also aid in the efficiency of incision. We define the angle ψ between the ice cliff and its backwasting ramp. ψ, as well as the ramp angle ϕ, are theoretically indicative of the efficiency of ice cliff incision and survival.

We first sought validation for our model of ice cliff backwasting and ramp scouring by investigating a time series of ArcticDEM data strips (Porter et al., 2022). The ArcticDEM is constructed from stereo pairs of WorldView and GeoEye satellite images, processed using "Surface Extraction by TIN-based Search space Minimization" to DEMs with 2 m horizontal resolution. For the years 2013 (July 15), 2014 (July 21), and 2017 (August 9), available DEM products covering Kennicott Glacier during the summer months of June-August were extracted using Google Earth Engine. These were then coregistered by minimizing the mean elevation difference between three patches of flat, stable, lightly vegetated glaciofluvial or moraine deposits in each DEM mosaic, applying a simple elevation offset to do so.

We then extracted topographic profiles for analysis of 100 ice cliffs and their associated backwasting ramps, using the NPS 2018 high resolution DEM (profile locations shown in Figure 1b-c). We sought to investigate differences in cliff-ramp geometry between stream-associated cliffs and non stream-associated cliffs, in the context of our geomorphic model. Ice cliffs were therefore categorized as those associated with streams and those with no associated streams. The stream channel prediction results were used to aid in this categorization but the presence of active stream action was confirmed in each case via visual identification of water flow or ice cliff undercutting visible in the orthophoto. Great care was taken in sampling the backwasting ramps, such that our sampling was not affecting by other disturbances such as surface collapses, debris movement, or other ice cliffs. The average slope of the ice cliff and ramp were then determined, along with the corresponding value of ψ between them.

3.3 Stream Discharge Measurements

We performed a series of discharge measurements to determine the ability of supraglacial streams to erode and transport debris. We selected a stream network exhibiting numerous examples of cliff-stream interactions for these measurements. We used the area-velocity method (Herschy, 1993) and nine measurements were performed at five locations (locations shown in Figure 1). Experiments took place during afternoon hours across three days in 2021 representing hot, sunny (July 13, 17) and cool, cloudy (July 14) weather conditions. Stream measurement locations were selected in reaches with linear, laminar flow and minimal turbulence. The length of sampled reaches varied between 1.5 and 8 m.

Two to three flow-transverse gates were defined for each discharge measurement and the channel cross section for each gate measured by hand using a measuring stick at 10 cm intervals. The area for each discharge measurement was then taken as the average of the area for the measured gates.

A neutrally buoyant mandarin orange was timed as it travelled in the stream between the flow-transverse gates. Individual measurements were removed from the analysis when the orange experienced undue turbulence or friction by interacting with eddies, the channel sidewall, or obstacles such as rocks in the stream bed. For each experiment 5-15 velocity measurements were made and averaged. Full information on individual reaches is summarized in Supplementary Table S1.

https://doi.org/10.5194/egusphere-2023-1913
Preprint. Discussion started: 26 September 2023

Average velocity across the gates is estimated at 0.9× the value of the measured velocity. This is consistent with low friction
130 stream bed such as an artificial channel or in this case bare ice (Rantz, 1982). The determined average velocity is then multiplied by the measured gate area to estimate discharge.

https://doi.org/10.5194/egusphere-2023-1913
Preprint. Discussion started: 26 September 2023

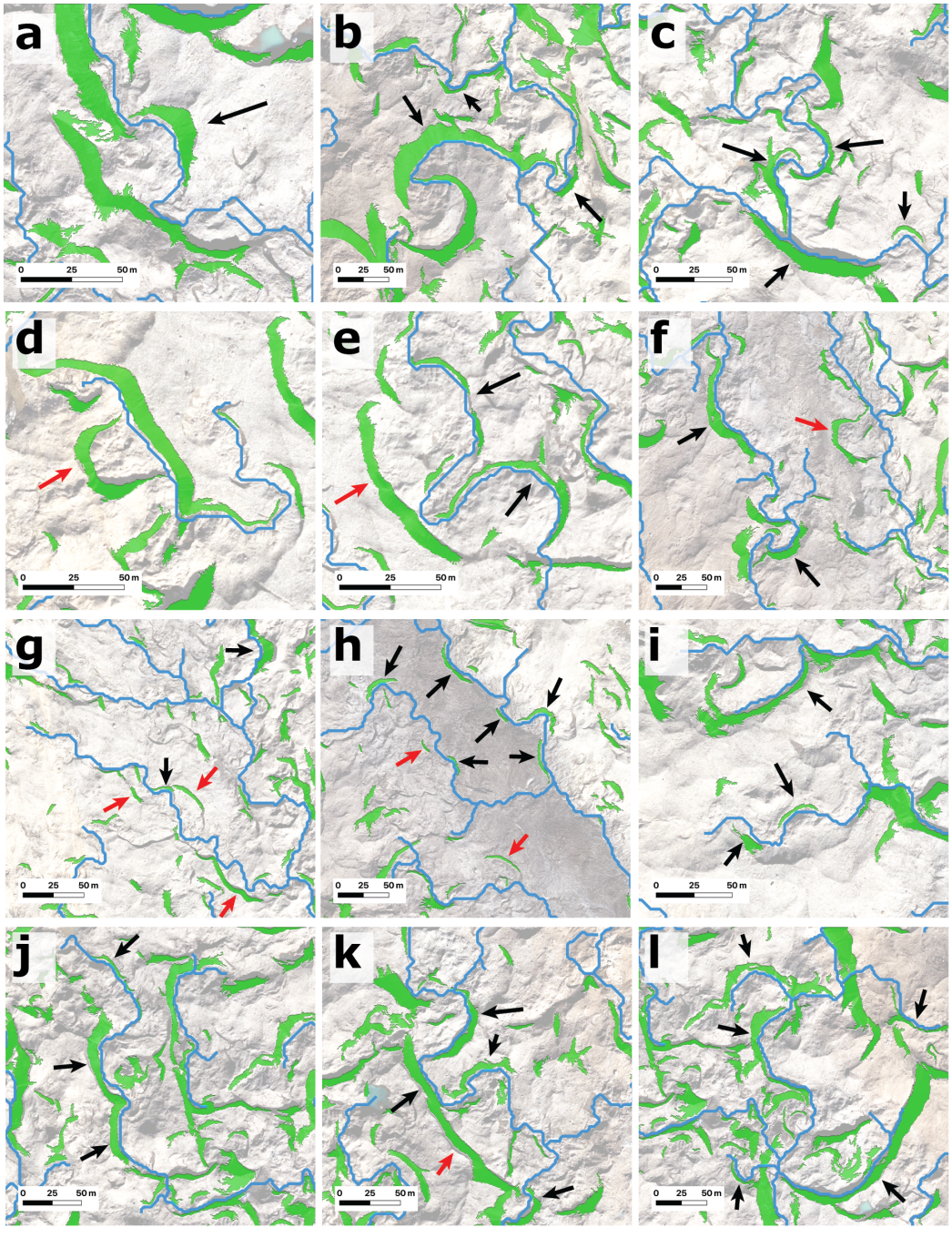

Figure 3. Examples of spatial relationships between identified ice cliffs (green) and stream channels (blue) mapped over a low-opacity orthophoto. Black arrows indicate curving ice cliff morphologies observed on the outside bend of supraglacial stream meanders; red arrows indicate similar ice cliff morphologies which appear to have been abandoned by stream channels.

https://doi.org/10.5194/egusphere-2023-1913
Preprint. Discussion started: 26 September 2023

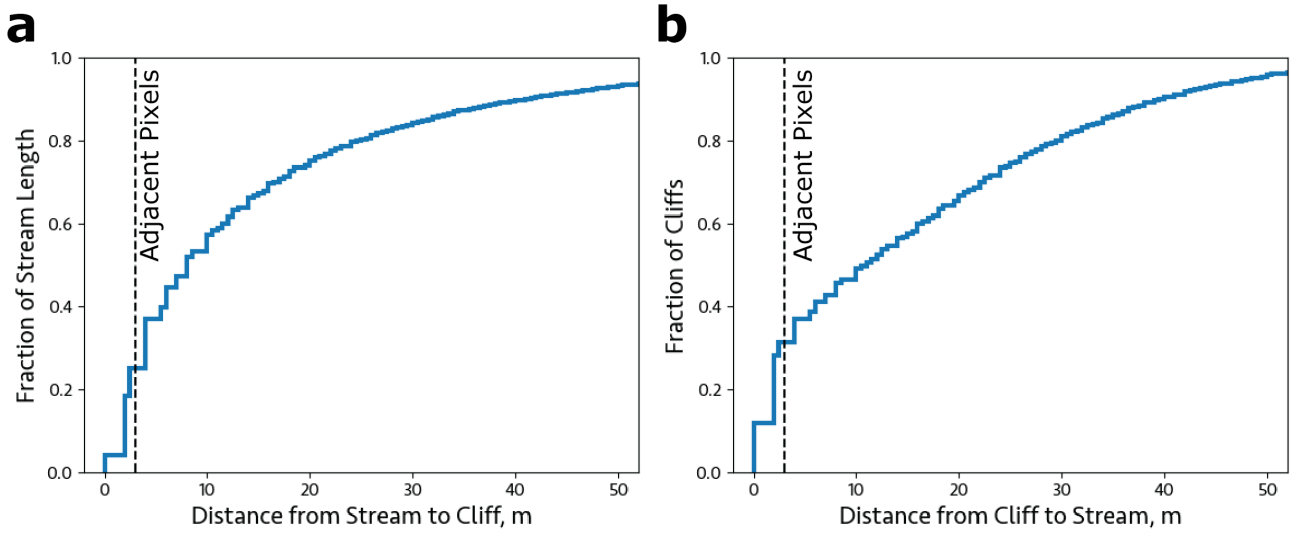

Figure 4. (a) Cumulative fraction of supraglacial stream length found within a given distance of identified ice cliffs. Threshold distance for adjacent DEM pixels is plotted. 23.8% of total stream length is directly adjacent to ice cliffs, while 50.6% is <10 m from ice cliffs. (b) Cumulative fraction of ice cliffs found within a certain distance of supraglacial streams; 31.4% of cliffs are directly adjacent to streams while 46.4% are within 10 m of streams.

4 Results

4.1 Ice cliff and stream mapping using photogrammetry

The automated ice cliff detection routine identified 12,667 ice cliffs with a total combined area, corrected for slope, of 5.53 km^2 (planform area 4.20 km^2). Ice cliffs thus account for 14.7% of the 37.2 km^2 sampled debris-covered surface (12.4% when ignoring slope in the area calculation). Median ice cliff surface area is 105 m^2 (IQR 45-290 m^2). Median cliff surface slope ranged from 32-54°. Cliffs were observed at all aspects, with broad peaks in the population facing NE and SW (Supplementary Figure S1).

A total of 5892 supraglacial stream channels were predicted, with lengths ranging from 4-1241 m and a total cumulative length of 51.9 km (average stream density 1.4 km km^{-2} for the study area). Average stream length was 88 m, with a standard deviation of 79 m, and median of 65 m (Supplementary Figure S1).

Predicted stream channel locations frequently coincide with the base of ice cliffs (Figures 3-4). 23.8% of total stream length is directly adjacent to ice cliffs, while 50.6% of stream length is within 10 m distance from the nearest ice cliff (median distance 8.9 m). Conversely, 31.4% of ice cliffs are directly adjacent to streams while 46.4% are within 10 m of streams, with a median distance of 11.3 m (Figure 4). Stream channel networks connect together numerous ice cliffs with sub-linear, sinuous, and crescent planform morphologies. Stream course meanders are frequently associated with distinctive crescent-shaped ice cliffs

https://doi.org/10.5194/egusphere-2023-1913
Preprint. Discussion started: 26 September 2023

on the outside of stream bends, reminiscent of cut banks on river channel systems in sedimentary environments. Examples of such ice cliffs are labelled in each panel of Figure 3 with black arrows. Crescent ice cliffs are also frequently observed at a distance of some tens of meters from predicted stream channels (labelled in each panel of Figure 3 with red arrows), inferring
150 a historical connection to the stream channel system.

https://doi.org/10.5194/egusphere-2023-1913
Preprint. Discussion started: 26 September 2023

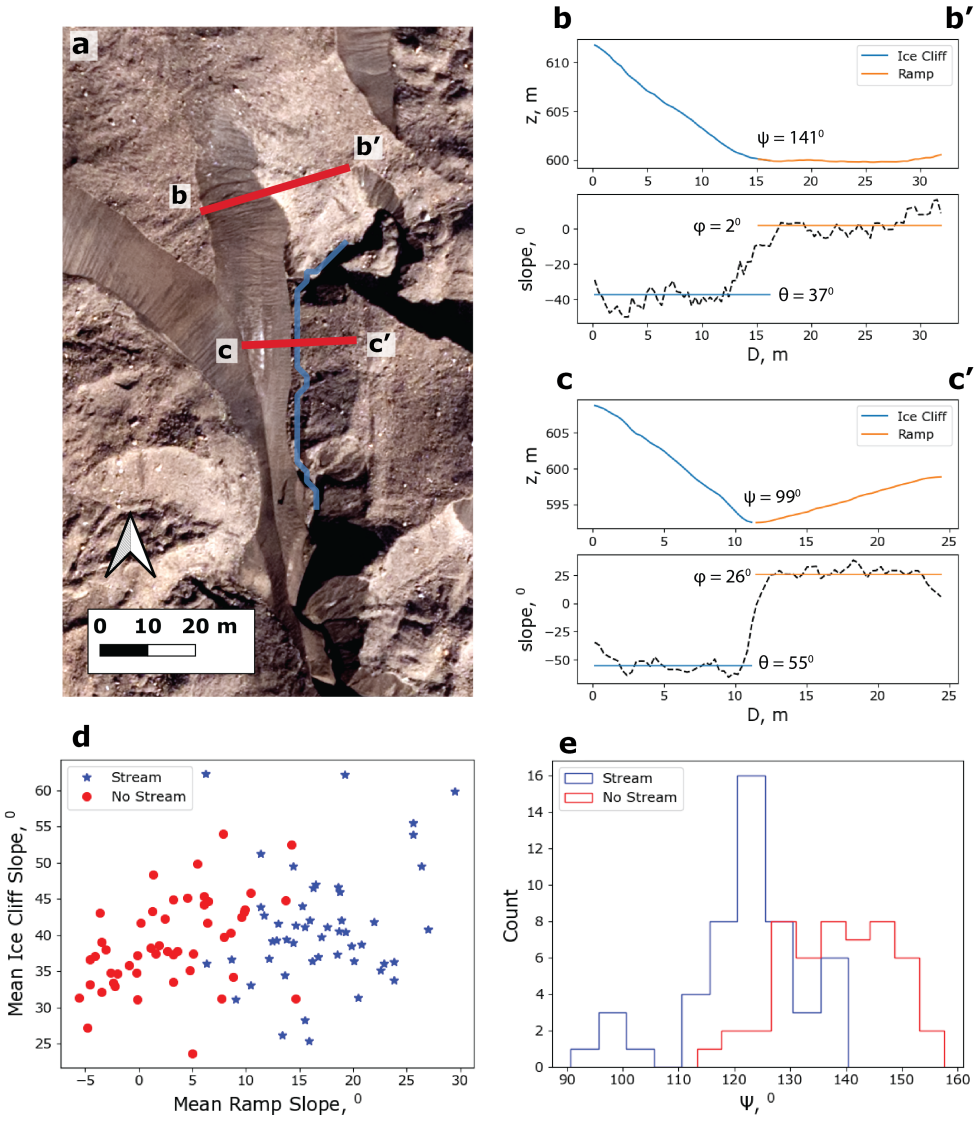

Figure 5. Ice cliff backwasting ramp analysis. (a) Orthoimage illustrating the location of profiles b-b' and c-c' on an ice cliff which experiences partial undercutting by a supraglacial stream. (b) Topographic profile over the ice cliff and backwasting ramp where it is unaffected by the supraglacial stream, resulting in $\psi = 141°$. (c) Topographic profile where the ice cliff is undercut by the supraglacial stream, resulting in $\psi = 99°$. (d) Ice cliff slope θ plotted against ramp slope ϕ for 100 profiles of systems with and without associated streams. (e) Histograms of ψ values for ice cliffs with and without associated streams.

4.2 Geomorphic model of ice cliff backwasting

We selected a very large (~40 m tall) ice cliff in the stagnant ice zone of Kennicott Glacier to investigate ice cliff backwasting through time. This minimized the relative impact of surface change due to glacier flow-ice becomes stagnant 2.5 km from the

https://doi.org/10.5194/egusphere-2023-1913
Preprint. Discussion started: 26 September 2023

glacier terminus (Gardner et al., 2022; Anderson et al., 2021b). As shown in Figure 2b-c, the ice cliff can be seen backwasting and scouring out a ramp, in this case at an angle of ψ = 110 °, consistent with our geomorphic model. This ice cliff is unique among the large ice cliffs in Kennicott Glaciers' stagnant zone in that it has a supraglacial stream and debris covered ramp at its base, and not the surface of a supraglacial pond.

We sampled 100 cliff-ramp systems with roughly equal shares of cliffs with and without streams to investigate the impact of streams on the backwasting. Two example ice cliff - ramp profiles are shown in Figure 5a, taken from the same ice cliff. Profile b-b' is taken from a location where the cliff has no associated stream at its base; to the north of the profile the cliff appears to be in the process of reburial under debris. Profile c-c' is taken from a location where a supraglacial stream channel is predicted, and corroborated by geomorphic evidence in the presence of an incisional canyon that approaches and intersects the ice cliff from the east, as well as the sharp, likely undercut base of the cliff. Profile c-c' exhibits a sharper ψ value than b-b', due to both a steeper ice cliff and a much steeper backwasting ramp. The results show that ice cliffs with streams tend to have lower ψ values as a result of steeper ramp angles for ice cliffs with similar pitch (Figure 5d-e), providing evidence that supraglacial streams enhance the efficiency of ice cliff incision.

4.3 Stream Discharge

The cross-sectional area of individual stream discharge measurement gates ranged from 630-2480 cm^2, with stream widths between 57-150 cm and maximum depths up to 12-35 cm. The thalweg, or deepest part of the channel cross-section, was in nearly all cases located nearer to the channel wall contiguous with the base of ice cliffs (Figure 6c; Supplementary Figures S2-5). This is consistent with lateral stream meander towards ice cliff undercuts. Mean measured velocities ranged from 0.60-1.13 m s^{-1}. The resultant flow rates were determined between 0.06 - 0.21 m^3 s^{-1} (Figure 6).

The streams sampled in the discharge measurements tended to be nearly continuously ice-floored, with little-to-no sediment resting on the channel bottom. When observed, sediments tended to be small accumulations of fine gravels/coarse sands collected in hollows or as small highly mobile bedforms (ripples), or larger rocks protruding above the surface of the stream. These larger static rocks were avoided in discharge measurement location selection. The streams themselves tended to be highly turbid, with low visibility beyond 5-10 cm.

https://doi.org/10.5194/egusphere-2023-1913
Preprint. Discussion started: 26 September 2023

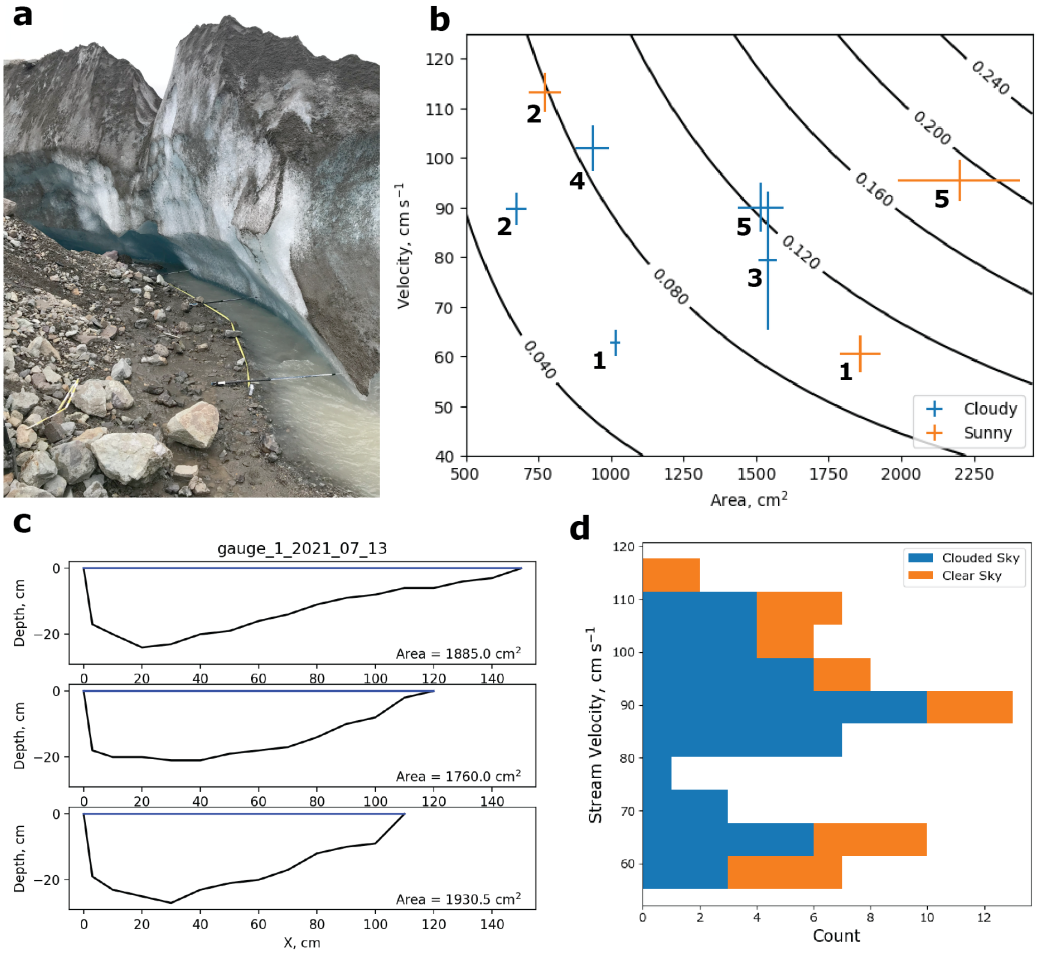

Figure 6. Results of stream discharge measurements. (a) Image of typical setup of discharge measurement including hiking poles marking the flux gates and tape measure. (b) Measured velocity and cross-sectional area for all discharge measurements; plotted contours are the resultant discharge in $m^3\ s^{-1}$. Data points are distinguished by measurement site (numerical labeling) and sunny/cloudy conditions (color). (c) Example of channel cross-sectional area measurements, from site 1 on July 13, 2021. (d) Histogram of measured velocity values from all 64 datapoints from 8 measurement sets.

https://doi.org/10.5194/egusphere-2023-1913
Preprint. Discussion started: 26 September 2023

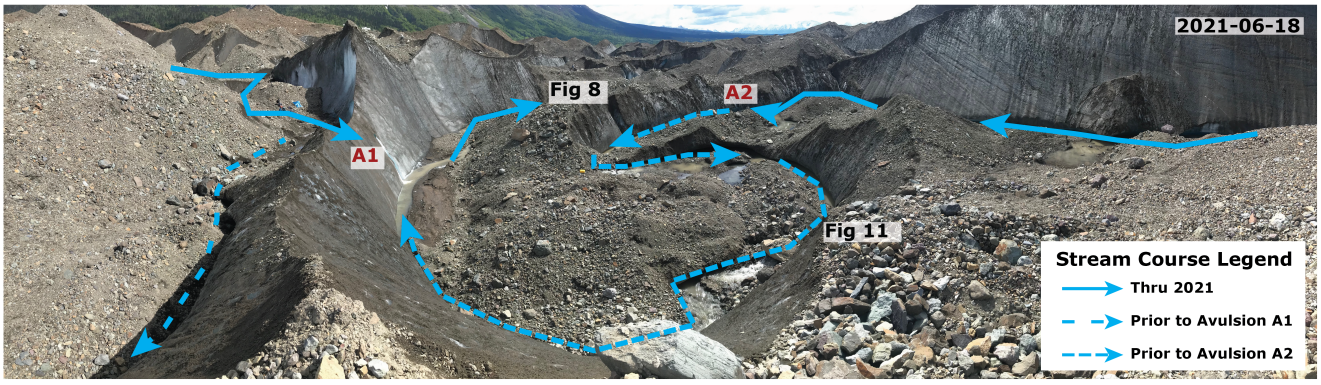

Figure 7. Perspective image of a large (40 m wide) topographic bowl bounded by a supraglacial stream meander undercutting associated ice cliffs. Observed stream courses and flow direction are displayed with the blue arrows. Dashed lines indicate stream courses abandoned following avulsions A1 (occurred sometime prior to June 18, 2021) and A2 (observed to occur on July 15, 2021). The locations of avulsions A1 and A2 are noted, as well as the locations of ice cliffs shown in Figures 8 and 11. Avulsion A2 resulted in stream flow directly into the page/downview of the camera.

Figure 8. Examples of stream undercuts of ice cliffs observed after avulsions; ablation stake and hiking pole for scale.

4.4 In situ geomorphic observations

In-situ observations find supraglacial streams frequently at the base of ice cliffs, consistent with remote sensing results (Figures 3, 7). Streams undercut the ice cliffs through lateral meandering and incision. Abandoned stream channels reveal up to >2.5 m horizontal and >1 m vertical incision (Figure 8a-b). In the case of repeated incision by multiple episodes of stream meander action, up to 3.5 m total vertical incision was observed, a significant local contribution to the total area of ice cliffs (Figure 8c).

There are also observed examples in which the action of supraglacial runoff contributes to ice cliff generation. Small rivulets of runoff, generated by the melt from ice cliffs and/or catchments of debris-covered ice, produce local incision and meanders as they travel through the supraglacial debris layer. This small scale incision generates ice exposures on the order of centimeters to tens of centimeters in height which have the potential to grow into much larger scale ice cliffs. In one dramatic example, a

https://doi.org/10.5194/egusphere-2023-1913
Preprint. Discussion started: 26 September 2023

time lapse camera used in fieldwork was knocked over by the generation and backwasting of an ice cliff that grew from 10 cm height cut by a rivulet to 1 m height and independent of the original runoff system within 38 days (Figure 9).

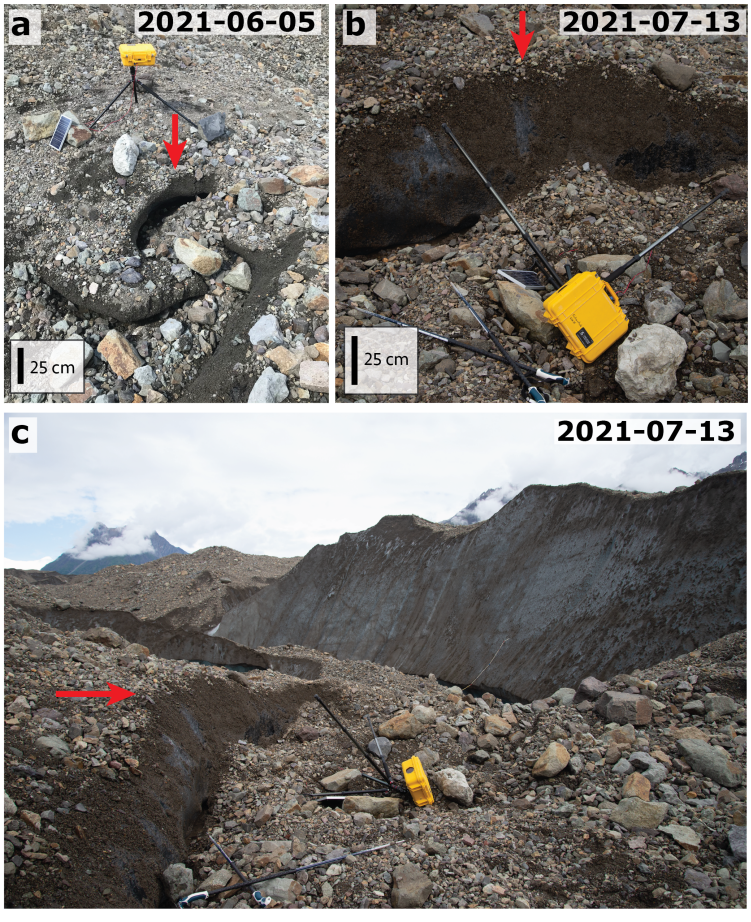

Figure 9. Field evidence for the role of hydrology in generating ice cliffs. (a) Time lapse camera installation observed on June 5, 2021. Red arrow indicates the crest of a short (10-20 cm tall) ice exposure associated with the incision of minor supraglacial drainage within the debris layer. The natural meander in drainage is expressed in the shape of the ice exposure (b-c) By July 13, 2021, the ice exposure had grown substantially into a small ice cliff 1 m tall and several meters wide, backwasting through the topography and knocking over the time lapse camera. This also illustrates the need for careful evaluation of local terrain features when placing instruments on the surface of debris-covered glaciers.

The impacts of two supraglacial stream avulsion events on ice cliffs were directly observed on Kennicott Glacier in the summers 2021 and 2022 (Figures 7, 10). These avulsions, i.e., rapid abandonments of the stream channel and formation of new channels, took place as a result of stream meanders in the same stream course system approaching each other from opposite directions, in manner similar to oxbow lake production in meandering river systems. As the stream meanders approach each other, the ice cliffs associated with the cut bank side of the meander meet, producing an ice fin with a sharp crest. Once the ice

https://doi.org/10.5194/egusphere-2023-1913
Preprint. Discussion started: 26 September 2023

fin thins sufficiently the upstream meander breaks through and the stream avulsion occurs, abandoning the prior stream path between those two points. Rapid stream flow at the avulsion point leads to accelerated collapse of the ice fin. In some cases, stream undercutting can contribute to mechanical collapse of ice cliffs and fins as well.

Channels abandoned by stream avulsion events initially reveal the extent of stream incision under ice cliffs. However, the shape of the overhang eventually melts out and in many cases the ice cliff begins to be reburied under debris. This was observed for south-facing ice cliffs following avulsion A2 on July 15, 2021 (Figure 11). Equator-facing ice cliffs are generally not expected to persist due to the effects of differential insolation-driven ablation leading them to be flattened and reburied (Buri and Pellicciotti, 2018). Thus it is reasonable to infer that stream action at the base of ice cliffs is sufficient to maintain the cliff's survival, counteracting ablation-driven flattening.

Figure 10. Examples of supraglacial stream avulsions and undercutting resulting in ice cliff collapse. (a) Avulsions A1 (occurred sometime prior to June 18, 2021), with stream flow boring through thinning ice cliff fin. (b-c) Avulsion A2 (observed to occur on July 15, 2021). Thinning of the ice cliff fin and lateral stream migration resulted in rapid ice cliff collapse and stream avulsion. (d-e) Observed ice cliff collapses associated with stream undercutting, (d) on the ground, and (e) observed in photogrammetry data.

https://doi.org/10.5194/egusphere-2023-1913
Preprint. Discussion started: 26 September 2023

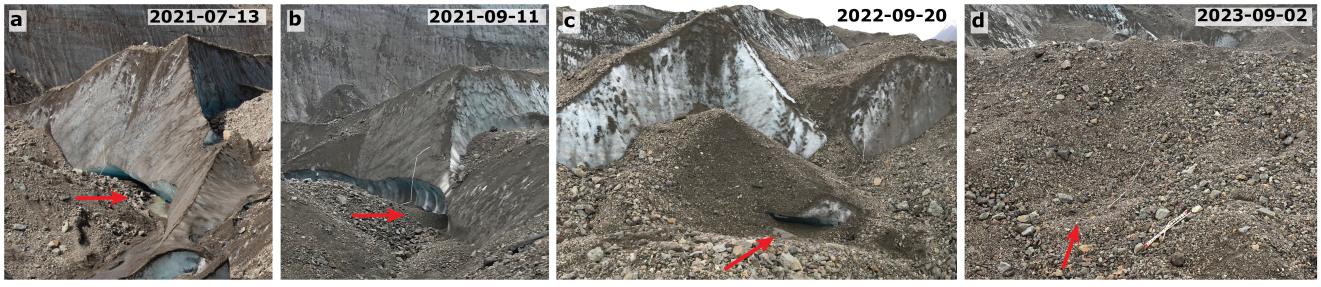

Figure 11. Observed reburial of south-facing ice cliff under debris following stream channel abandonment. (a) Ice cliff with active supraglacial stream at its base, providing undercutting via lateral meandering. Base of cliff is unburied. (b) After avulsion A2 (Figure 10), undercutting ceases and undercut overhang begins to melt out. (c) After complete melting of the undercut shape, the ice cliff begins to be reburied under debris. (d) Complete reburial of the former ice cliff area under debris 1 year after supraglacial stream avulsion.

5 Discussion

5.1 Geomorphic Relationship Between Ice Cliffs and Streams

It is clear from the results of our DEM analysis that supraglacial streams and ice cliffs have a strong relationship in terms of spatial proximity and geomorphology. Linear to crescent-shaped cliffs are often observed with a supraglacial stream at their base or within tens of meters. Half of observed streams by length are within 10 m of ice cliffs and 31.4% of ice cliffs have supraglacial streams directly at their base. Kneib et al. (2023) determined that 38.9% of ice cliffs in High Mountain Asia are stream-influenced, defined as being within 40 m of supraglacial streams. If we applied this broad threshold to our analysis, 89.9% of ice cliffs on Kennicott Glacier are stream-influenced. Conservatively, one third to one half of ice cliffs on Kennicott Glacier are stream-influenced. These cliffs typically follow the arc of supraglacial stream meanders on the outside of stream bends, analagous to cut banks in sedimentary river systems. This morphology is likely indicative of ice cliffs that have hydrological processes as their primary control.

Supraglacial streams act on the surface of the glacier through two processes: thermoerosional incision of the ice and the erosion/transport of supraglacial debris. Karlstrom et al. (2013) showed that because heat transfer between the stream flow and ice channel walls is dependent on turbulence in a similar fashion to sediment transport, supraglacial streams produce meanders with a very similar planform geometry to alluvial rivers. This lateral as well as vertical thermoerosional incision allows streams to carve new ice cliffs into the glacier surface (Figure 9), as well as undercut and enhance the incision of existing ice cliffs (Figure 8). Indeed, we have shown evidence from our geomorphic model that the presence of streams measurably enhances the incision of ice cliffs into the glacier surface, aiding in ice cliff survival. More pronounced lateral migration of streams under ice cliffs leads to more exposed ice and enhanced backwasting at the ice cliff base, as well as possible mechanical collapse (Figure 10). This is the mechanism by which stream channel meanders may control the morphology of ice cliffs, evolving crescent-shaped cliffs on their outside bends.

https://doi.org/10.5194/egusphere-2023-1913
Preprint. Discussion started: 26 September 2023

Crescent cliffs adjacent to supraglacial stream systems often appear to be formerly associated with stream channel meanders, in a manner reminiscent of oxbow lakes adjacent to sedimentary river systems (Fisk, 1947). Observation of multiple stream avulsion events during 2021 fieldwork confirmed that stream abandonment of ice cliffs occurs, due to both meander pinch-off or lateral migration. These streams leave behind ice cliffs with a morphology formerly influenced by stream action. Ice cliffs abandoned by streams lose the undercut morphology at their base and may be re-buried by debris, particularly if they are equator-facing (Figure 11; Buri and Pellicciotti (2018)). This observation further underlines the importance of streams to ice cliff survival.

5.2 Stream Erosion of Sediments at the Base of Ice Cliffs

In sediment-bedded streams, the ability of the stream to erode (mobilize from rest), transport (carry within the flow), or deposit (drop out of the flow) clasts of a given size as a function of stream velocity has historically been described by a set of empirical relationships illustrated by the Hjulstrom curve (Hjulström (1935); Supplementary Figure S6). Comparison of our discharge measurement results to this diagram suggests the ability to erode debris clasts up to 1 cm in size and transport debris up to 10 cm in size.

However, because our supraglacial streams are generally bedded by ice and not sediment, the Hjulstrom diagram may be ill-suited for estimation of the debris erosion/mobilization threshold. If we assume a smooth ice-floored stream bed, we can predict the onset of sediment transport (erosion) with a simple force balance. We may consider the drag force F_{drag} required to overcome the static frictional force $F_{friction}$ of a debris clast resting on the ice in a stream channel:

$$F_{drag} = \frac{AC_w\rho_{water}v_{flow}^2}{2} \tag{1}$$

$$F_{friction} = \mu F_N = \mu\rho_{rock}V_{rock}g \tag{2}$$

where A is the cross sectional area of the rock orthogonal to flow direction, C_w is the drag coefficient, ρ_{water} and ρ_{rock} the densities of water and rock, v_{flow} the stream velocity, μ the static coefficient of friction (0.05 for ice near 0°C (Mills, 2008)), F_N the normal force, V_{rock} the rock volume, and g acceleration due to gravity. At the critical drag force, $F_{drag} = F_{friction}$, we can determine the maximum size of rock of a certain shape that is mobilized by the flow.

We assumed a rock density of 2700 kg m^{-3} and used a half-sphere (C_w = 0.42) and a cube (C_w = 1.05) (Sighard F. Hoerner, 1965) as end member shapes to calculate the diameter of debris clasts our measured stream velocities are capable of mobilizing. We found our measured velocities (0.6 - 1.13 m s^{-1}) capable of moving rocks up to 9-30 cm (half-sphere) and 14-51 cm (cube) in diameter. These values match or exceed our measured channel depths.

These results are consistent with the fact that little static sediment accumulation is observed in the measured stream channels. Where observed, static sediment size is typically the order of or larger than the stream depth, or it is gravel and sand collected in hollows in the rough stream bed (our force balance assumes a smooth bed). Clasts larger than stream channel depth have also been observed in motion in ice-bedded streams.

https://doi.org/10.5194/egusphere-2023-1913
Preprint. Discussion started: 26 September 2023

This analysis thus supports that supraglacial streams are highly effective at removing debris from the base of ice cliffs, which may aid in preventing their reburial. The relative importance of debris erosion and transport in comparison to thermoerosional undercutting of the ice cliff face is unknown.

5.3 Feedbacks and considerations for other debris-covered glacier surfaces

Because ice cliffs contribute significantly to melt runoff, there is additionally the opportunity for a feedback loop between ice cliffs and streams. More exposed ice cliff area leads to higher flow and incision rates with more power to create and maintain ice cliffs. Greater debris thickness leads to a higher differential melt between sub-debris and ice cliff melt rates, increasing the relative importance of such a feedback. At the same time, lower sub-debris melt rates leads to significantly reduced runoff from catchment areas without ice cliffs and a reduced ability of runoff to generate new cliffs.

Thicker debris or debris with larger clasts (greater than tens of cm or significantly deeper than stream depth) will also be less effectively removed from ice cliffs' bases and will be more likely to fill in stream undercuts. This will in general reduce the ability of runoff streams to generate new ice cliffs and maintain existing ice cliffs.

While this study is focused on investigating the processes by which supraglacial streams control ice cliff formation and change, there are a number of other processes which also have major impacts on ice cliffs. Glacial hydrology in general can impact ice cliffs through other processes. The collapse of englacial conduits may lead to ice cliff production as a result of the exposure of former conduit walls (Mölg et al., 2020). Supraglacial ponds often are rimmed in part by ice cliffs (Scott Watson et al., 2017; Steiner et al., 2019), with the pond playing a key role in altering ice cliff surface energy balance and undercutting through enhanced subaquous melt rates (Miles et al., 2016). Ice cliffs may also be generated through the modification of crevasse walls. Kneib et al. (2023) used geomorphic relationships to determine that supraglacial streams, crevasses, and supraglacial ponds are the primary controls on ice cliffs in High Mountain Asia, in order of decreasing importance.

On Kennicott Glacier supraglacial streams are prevalent across the majority of the active portion of the debris-covered tongue. The importance of streams are diminished (1) where active crevassing occurs and runoff is thus sent rapidly to the englacial system via moulin production or (2) where stagnant ice results in flattened surface topography and the dominance of supraglacial ponds.

Crevassing was observed on Kennicott Glacier's western terminus in the vicinity of a re-advance that peaked around 2018 (see Supplementary Text S1, Video S3, and Figure S7), resulting in ice dynamics dominating over hydrology in driving ice cliff change for this locale on the glacier. At Kennicott Glacier, the ice becomes stagnant 2.5 km from its terminus at an elevation of 500 m.a.s.l. (Gardner et al., 2022; Anderson et al., 2021b); below this elevation streams are rare and ponds are dominant, while above this elevation streams are more common.

A number of other studies have noted a close geospatial linkage between supraglacial streams and ice cliffs on other glaciers around the world, including Zmuttgletscher (Mölg et al., 2020), Trakarding Glacier (Sato et al., 2021), and glaciers in High Mountain Asia (Kneib et al., 2023). Our work shows the processes by which streams contribute to ice cliff maintenance and production at Kennicott Glacier; these processes are likely universal and applicable to other debris-covered glaciers such as those listed above.

https://doi.org/10.5194/egusphere-2023-1913
Preprint. Discussion started: 26 September 2023

6 Conclusions

We have shown the importance of supraglacial streams in providing a feedback and control on ice cliff formation, dynamics, and survival on the debris-covered Kennicott Glacier. The incision of streams into the debris-covered glacier surface produces ice exposures that can grow into larger ice cliffs.

Streams running at the base of fully developed ice cliffs enhance the survivability of the ice cliff system through thermo-erosional incision of the ice, erosion of supraglacial debris which mass wastes to the base of the ice cliff, and undercutting of the ice cliff face. Undercutting of the ice face and erosion of debris prevents the ice cliff base from being re-buried by debris, while the undercut geometry increases exposed ice surface area available for melt. Streams in particular aid in the survival of ice cliffs that would otherwise disappear due to slope-aspect dependent radiation effects (Buri and Pellicciotti, 2018). We find that 31.4% of ice cliffs are actively influenced by streams while 46.4% are in close proximity ($<$10 m) to streams.

Stream meanders also control the morphology of ice cliffs, producing curving to crescent ice cliff shapes on the outer edge of stream meanders. Meander cut off stream avulsions result in the demise of ice cliffs due to collapse at the avulsion point as well as reburial under debris where ice cliffs are abandoned by stream systems.

Understanding the drivers of ice cliff formation and evolution will aid us in predicting how debris-covered glacier surfaces will change in the future, enhancing our understanding of melt, retreat, and discharge from these glaciers. Our study highlights specific drivers and feedbacks resulting from supraglacial hydrology that enhances our understanding of these systems. In the future, landscape evolution models may be developed to predict these dynamics and ultimately derive steady state ice cliff statistics for glaciers based on given climatic, glaciological, and debris-supply conditions.

Data availability. Data products produced by this study are stored in a data repository at Petersen et al. (2023).

Competing interests. We have no competing interests to declare.

Author contributions. Eric Petersen designed the study, led fieldwork data collection, carried out data analysis and drafted the manuscript. Regine Hock was Principal Investigator of the project, and contributed to development as well as manuscript editing. Michael Loso provided the photogrammetry dataset and contributed greatly to geomorphologic analysis/interpretation and manuscript writing.

Acknowledgements. The project was supported by NSF Award 1917536 (GLD). We thank field volunteers who made this work possible, including Cameron Markovsky, Julian Dann, Anna Thompson, Andrew Johnson, Nicole Trenholm, Brooke Kubby, Ruitang Yang, Kitrea Takata-Glushkoff, Maria Zeitz, Jason Geck, Harlan Loso, and Levi Williamson. We thank the Wrangell Mountains Center for their support during multiple field expeditions.

https://doi.org/10.5194/egusphere-2023-1913
Preprint. Discussion started: 26 September 2023

References

Anderson, L. S. and Anderson, R. S.: Modeling debris-covered glaciers: response to steady debris deposition, The Cryosphere, 10, 1105–1124, https://doi.org/https://doi.org/10.5194/tc-10-1105-2016, 2016.

Anderson, L. S., Armstrong, W. H., Anderson, R. S., and Buri, P.: Debris cover and the thinning of Kennicott Glacier, Alaska: in situ measurements, automated ice cliff delineation and distributed melt estimates, The Cryosphere, 15, 265–282, https://doi.org/https://doi.org/10.5194/tc-15-265-2021, publisher: Copernicus GmbH, 2021a.

Anderson, L. S., Armstrong, W. H., Anderson, R. S., Scherler, D., and Petersen, E.: The Causes of Debris-Covered Glacier Thinning: Evidence for the Importance of Ice Dynamics From Kennicott Glacier, Alaska, Frontiers in Earth Science, 9, https://www.frontiersin.org/article/10.3389/feart.2021.680995, 2021b.

Anderson, R. S.: A model of ablation-dominated medial moraines and the generation of debris-mantled glacier snouts, Journal of Glaciology, 46, 459–469, https://doi.org/10.3189/172756500781833025, publisher: Cambridge University Press, 2000.

Benn, D. I., Bolch, T., Hands, K., Gulley, J., Luckman, A., Nicholson, L. I., Quincey, D., Thompson, S., Toumi, R., and Wiseman, S.: Response of debris-covered glaciers in the Mount Everest region to recent warming, and implications for outburst flood hazards, Earth-Science Reviews, 114, 156–174, https://doi.org/10.1016/j.earscirev.2012.03.008, 2012.

Bhushan, S., Syed, T. H., Arendt, A. A., Kulkarni, A. V., and Sinha, D.: Assessing controls on mass budget and surface velocity variations of glaciers in Western Himalaya, Scientific Reports, 8, 8885, https://doi.org/10.1038/s41598-018-27014-y, number: 1 Publisher: Nature Publishing Group, 2018.

Bolch, T., Kulkarni, A., Kääb, A., Huggel, C., Paul, F., Cogley, J. G., Frey, H., Kargel, J. S., Fujita, K., Scheel, M., Bajracharya, S., and Stoffel, M.: The State and Fate of Himalayan Glaciers, Science, 336, 310–314, https://doi.org/10.1126/science.1215828, publisher: American Association for the Advancement of Science, 2012.

Bozhinskiy, A. N., Krass, M. S., and Popovnin, V. V.: Role of Debris Cover in the Thermal Physics of Glaciers, Journal of Glaciology, 32, 255–266, https://doi.org/10.3189/S0022143000015598, publisher: Cambridge University Press, 1986.

Buri, P. and Pellicciotti, F.: Aspect controls the survival of ice cliffs on debris-covered glaciers, Proceedings of the National Academy of Sciences, 115, 4369–4374, https://doi.org/10.1073/pnas.1713892115, 2018.

Buri, P., Miles, E. S., Steiner, J. F., Ragettli, S., and Pellicciotti, F.: Supraglacial Ice Cliffs Can Substantially Increase the Mass Loss of Debris-Covered Glaciers, Geophysical Research Letters, 48, e2020GL092 150, https://doi.org/https://doi.org/10.1029/2020GL092150, _eprint: https://agupubs.onlinelibrary.wiley.com/doi/pdf/10.1029/2020GL092150, 2021.

Cogley, J. G., Hock, R., Rasmussen, L. A., Arendt, A. A., Bauder, A., Braithwaite, R. J., Jansson, P., Kaser, G., Möller, M., Nicholson, L., and Zemp, M.: Glossary of glacier mass balance and related terms, IHP-VII Technical Documents in Hydrology, 86, https://doi.org/10.5167/uzh-53475, num Pages: 114 Place: Paris Publisher: UNESCO/IHP, 2011.

Dolgushin, L.: Vliyaniye eolovoy zapylennosti lednikov i poverkhnostnoy moreny na tayaniye lednikov Sredney Azii. [The influence of aeolian dusting of glaciers and superficial moraine on glacier thawing in Central Asia), Materialy Glyatsiologicheskikh Issledovaniy. Khronika. Obsuzhdeniya, 20, 108–116, 1972.

Fisk, H. N.: Fine-grained alluvial deposits and their effects on Mississippi River activity, Technical Reports, Waterways Experiment Station (U.S.). United States, Mississippi River Commission, https://usace.contentdm.oclc.org/digital/collection/p266001coll1/id/9658/, 1947.

Gardelle, J., Berthier, E., Arnaud, Y., and Kaab, A.: Region-wide glacier mass balances over the Pamir-Karakoram-Himalaya during 1999-2011 (vol 7, pg 1263, 2013), The Cryosphere, 7, 1885–1886, https://doi.org/10.5194/tc-7-1885-2013, publisher: Copernicus, 2013.

https://doi.org/10.5194/egusphere-2023-1913
Preprint. Discussion started: 26 September 2023

Gardner, A. S., Fahnestock, M. A., and Scambos, T. A.: MEaSUREs ITS_LIVE Landsat Image-Pair Glacier and Ice Sheet Surface Velocities, Version 1, https://doi.org/https://doi.org/10.5067/IMR9D3PEI28U, 2022.

Herreid, S. and Pellicciotti, F.: Automated detection of ice cliffs within supraglacial debris cover, The Cryosphere, 12, 1811–1829, https://doi.org/https://doi.org/10.5194/tc-12-1811-2018, publisher: Copernicus GmbH, 2018.

Herschy, R.: The velocity-area method, Flow Measurement and Instrumentation, 4, 7–10, https://doi.org/10.1016/0955-5986(93)90004-3, 1993.

Hjulström, F.: Studies of the morphological activity of rivers as illustrated by the River Fyris, http://urn.kb.se/resolve?urn=urn:nbn:se:uu:diva-481786, publisher: The Geological institution of the University of Upsala, 1935.

Karlstrom, L., Gajjar, P., and Manga, M.: Meander formation in supraglacial streams: MEANDERING SUPRAGLACIAL STREAMS, Journal of Geophysical Research: Earth Surface, 118, 1897–1907, https://doi.org/10.1002/jgrf.20135, 2013.

Khodakov, V.: Raschet i prognoz ablyatsii morenosoderzhashchego l'da. [Calculation and prognosis of debris-containing ice ablation)., Materialy Glyatsiologicheskikh Issledovaniy. Khronika. Obsuzhdeniya, 20, 215–218, 1972.

Kneib, M., Fyffe, C. L., Miles, E. S., Lindemann, S., Shaw, T. E., Buri, P., McCarthy, M., Ouvry, B., Vieli, A., Sato, Y., Kraaijenbrink, P. D. A., Zhao, C., Molnar, P., and Pellicciotti, F.: Controls on Ice Cliff Distribution and Characteristics on Debris-Covered Glaciers, Geophysical Research Letters, 50, e2022GL102 444, https://doi.org/10.1029/2022GL102444, _eprint: https://onlinelibrary.wiley.com/doi/pdf/10.1029/2022GL102444, 2023.

Kääb, A., Berthier, E., Nuth, C., Gardelle, J., and Arnaud, Y.: Contrasting patterns of early twenty-first-century glacier mass change in the Himalayas, Nature, 488, 495–498, https://doi.org/10.1038/nature11324, 2012.

Mattson, L., Gardner, J., and Young, G.: Ablation on Debris Covered Glaciers: an Example from the Rakhiot Glacier, Punjab, Himalaya, Intern. Assoc. Hydrol. Sci., 218, 298–296, https://www.semanticscholar.org/paper/Ablation-on-Debris-Covered-Glaciers%3A-an-Example-the-Mattson-Gardner/4c21834c00857f5d1e329e4bf86df6e4b28e2fc0, 1993.

Maurer, J. M., Schaefer, J. M., Rupper, S., and Corley, A.: Acceleration of ice loss across the Himalayas over the past 40 years, Science Advances, 5, eaav7266, https://doi.org/10.1126/sciadv.aav7266, 2019.

Miles, E. S., Pellicciotti, F., Willis, I. C., Steiner, J. F., Buri, P., and Arnold, N. S.: Refined energy-balance modelling of a supraglacial pond, Langtang Khola, Nepal, Annals of Glaciology, 57, 29–40, https://doi.org/10.3189/2016AoG71A421, 2016.

Mills, A.: The coefficient of friction, particularly of ice, Physics Education, 43, 392, https://doi.org/10.1088/0031-9120/43/4/006, 2008.

Moore, P. L.: Numerical Simulation of Supraglacial Debris Mobility: Implications for Ablation and Landform Genesis, Frontiers in Earth Science, 9, https://www.frontiersin.org/articles/10.3389/feart.2021.710131, 2021.

Mölg, N., Ferguson, J., Bolch, T., and Vieli, A.: On the influence of debris cover on glacier morphology: How high-relief structures evolve from smooth surfaces, Geomorphology, 357, 107 092, https://doi.org/10.1016/j.geomorph.2020.107092, 2020.

NASA/METI/AIST/Japan Spacesystems and U.S./Japan ASTER Science Team: ASTER Global Digital Elevation Model V003 [Data set], https://doi.org/https://doi.org/10.5067/ASTER/ASTGTM.003, 2019.

Pellicciotti, F., Stephan, C., Miles, E., Herreid, S., Immerzeel, W. W., and Bolch, T.: Mass-balance changes of the debris-covered glaciers in the Langtang Himal, Nepal, from 1974 to 1999, Journal of Glaciology, 61, 373–386, https://doi.org/10.3189/2015JoG13J237, 2015.

Petersen, E., Hock, R., and Loso, M.: Data Products associated with "Stream hydrology controls on ice cliff generation, evolution, and survival on debris-covered glaciers", https://doi.org/10.5281/zenodo.8373145, 2023.

https://doi.org/10.5194/egusphere-2023-1913
Preprint. Discussion started: 26 September 2023

Porter, C., Howat, I., Noh, M.-J., Husby, E., Khuvis, S., Danish, E., Tomko, K., Gardiner, J., Negrete, A., Yadav, B., Klassen, J., Kelleher, C., Cloutier, M., Bakker, J., Enos, J., Arnold, G., Bauer, G., and Morin, P.: ArcticDEM - Strips, Version 4.1, https://doi.org/10.7910/DVN/C98DVS, 2022.

Rantz, S. E.: Measurement and computation of streamflow, USGS Numbered Series 2175, U.S. G.P.O., https://doi.org/10.3133/wsp2175, code Number: 2175 Code: Measurement and computation of streamflow Publication Title: Measurement and computation of streamflow Reporter: Measurement and computation of streamflow Series: Water Supply Paper, 1982.

RGI Consortium: Randolph Glacier Inventory - A Dataset of Global Glacier Outlines: Version 6.0: Technical Report, Tech. rep., Global Land Ice Measurements from Space, Colorado, USA, https://doi.org/10.7265/N5-RGI-60, 2017.

Sakai, A., Nakawo, M., and Fujita, K.: Distribution Characteristics and Energy Balance of Ice Cliffs on Debris-covered Glaciers, Nepal Himalaya, Arctic, Antarctic, and Alpine Research, 34, 12–19, https://doi.org/10.1080/15230430.2002.12003463, 2002.

Sato, Y., Fujita, K., Inoue, H., Sunako, S., Sakai, A., Tsushima, A., Podolskiy, E. A., Kayastha, R., and Kayastha, R. B.: Ice Cliff Dynamics of Debris-Covered Trakarding Glacier in the Rolwaling Region, Nepal Himalaya, Frontiers in Earth Science, 9, https://www.frontiersin.org/articles/10.3389/feart.2021.623623, 2021.

Scherler, D., Wulf, H., and Gorelick, N.: Global Assessment of Supraglacial Debris-Cover Extents, Geophysical Research Letters, 45, 11,798–11,805, https://doi.org/10.1029/2018GL080158, _eprint: https://agupubs.onlinelibrary.wiley.com/doi/pdf/10.1029/2018GL080158, 2018.

Scott Watson, C., Quincey, D. J., Carrivick, J. L., and Smith, M. W.: Ice cliff dynamics in the Everest region of the Central Himalaya, Geomorphology, 278, 238–251, https://doi.org/10.1016/j.geomorph.2016.11.017, 2017.

Sighard F. Hoerner: Fluid-Dynamic Drag, http://archive.org/details/FluidDynamicDragHoerner1965, 1965.

Steiner, J. F., Buri, P., Miles, E. S., Ragettli, S., and Pellicciotti, F.: Supraglacial ice cliffs and ponds on debris-covered glaciers: spatio-temporal distribution and characteristics, Journal of Glaciology, 65, 617–632, https://doi.org/10.1017/jog.2019.40, publisher: Cambridge University Press, 2019.

Østrem, G.: Ice Melting under a Thin Layer of Moraine, and the Existence of Ice Cores in Moraine Ridges, Geografiska Annaler, 41, 228–230, http://www.jstor.org/stable/4626805, 1959.